Volume 10
Number 22
14 June 2022
Pages 4119–4322

Journal of Materials Chemistry B

Materials for biology and medicine

rsc.li/materials-b

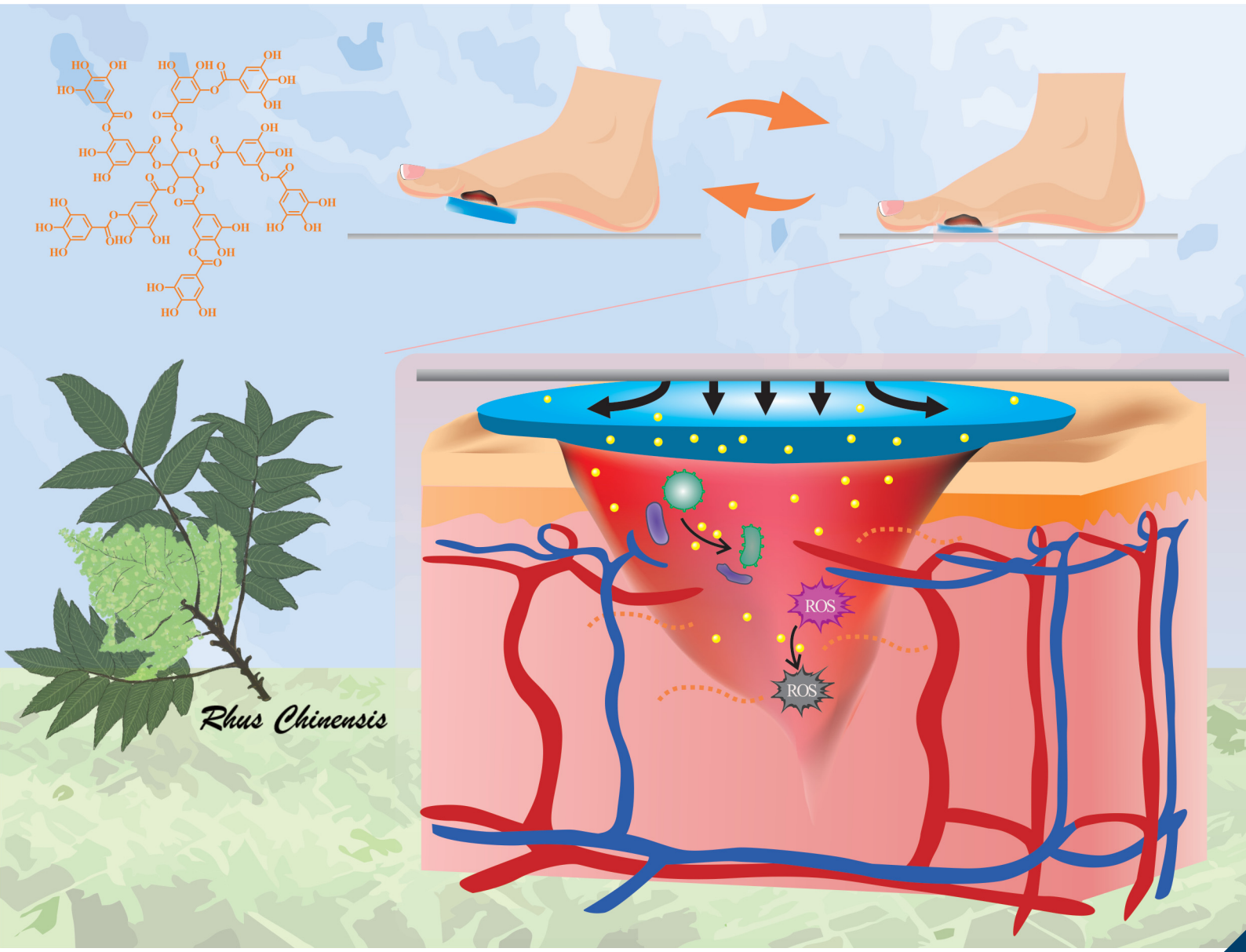

ISSN 2050-750X

ROYAL SOCIETY OF CHEMISTRY

PAPER

Donglei Liu, Rong Wang *et al.*
Tannic acid-reinforced zwitterionic hydrogels with multi-functionalities for diabetic wound treatment

Journal of Materials Chemistry B

ROYAL SOCIETY OF CHEMISTRY

PAPER

View Article Online
View Journal | View Issue

Cite this: J. Mater. Chem. B, 2022, 10, 4142

Tannic acid-reinforced zwitterionic hydrogels with multi-functionalities for diabetic wound treatment†

Kun Fang,‡[ab] Qinwei Gu,‡[ab] Mingzhu Zeng,[a] Zhimao Huang,[a] Haofeng Qiu,[c] Jiru Miao,[a] Yue Fang,[a] Yinyu Zhao,[a] Ying Xiao,[a] Ting Xu,[a] Robert Petrovich Golodok,[d] Vadim Victorovich Savich,[d] Alexander Phyodorovich Ilyushchenko,[d] Fanrong Ai,[b] Donglei Liu*[b] and Rong Wang*[a]

Received 4th November 2021,
Accepted 23rd April 2022

DOI: 10.1039/d1tb02413b

rsc.li/materials-b

Diabetic wounds remain one of the most prevalent hard-to-heal wounds in the clinic. The causative factors impeding the wound healing process include not only the elevated oxidative stress and bacterial infections but also the high and repetitive plantar stress (including compressive pressure and shear stress). Conventional hydrogel dressings are mechanically weak and fragile, limiting their applications in the high stress-loading conditions of diabetic foot ulcers. As such, mechanically tough hydrogel dressings with appropriate bioactivities are highly desirable for diabetic wound treatment. In this study, a mechanically reinforced hydrogel with multiple biofunctionalities was developed *via* a facile and straightforward strategy of incorporation of tannic acid (TA) in zwitterionic poly(sulfobetaine methacrylate) (polySBMA) hydrogel. The polySBMA hydrogel reinforced by TA showed excellent mechanical property, with the tensile stress and compressive stress up to 93.7 kPa and 18.4 MPa, respectively, and it could resist cyclic compressive stress at ~200 kPa (maximum in-shoe plantar pressure) for up to 3500 cycles. The TA-reinforced zwitterionic hydrogel exhibited strong adhesion to skin tissue (20.2 kPa), which was expected to reduce the shear stress on the foot. The plantar pressure on the foot was significantly reduced by the application of the resilient hydrogel. Attributed to the antioxidant and antibacterial properties of TA, the hydrogel showed rapid radical scavenging capability and strong bactericidal efficacy against Gram-positive and Gram-negative bacteria. *In vitro* and *in vivo* studies confirmed that the hydrogel has good cytocompatibility and negligible skin irritation, and promoted healing of diabetic wounds in mice. Such tough and effective hydrogel with a straightforward preparation strategy holds great promise as wound dressings for diabetic wound treatment.

1 Introduction

Diabetes is becoming a severe disease affecting about 422 million people globally.[1] Wound ulcers are common but severe complications among diabetic patients, with a lifetime incident rate of 19–34% and a recurrence rate of ~40%.[2] Without appropriate intervention, minor traumas on the foot of diabetic patients caused by cutting, abrasion, or squeezing can develop into serious wound ulcers and lead to amputation or even death. Repetitive and excessive plantar stress, oxidative stress effect, and bacterial infection are recognized as the main reasons for the poor recovery rate and high recurrent rate of diabetic wounds.[2] Thus, relieving excessive stress, reducing oxidative effect, and inhibiting bacterial infections are important measures in the treatment of diabetic wounds and prevention of their recurrence.

Hydrogel has been one of the promising wound dressings due to its good moisture retention capability, biocompatibility, and tunable bioactivity.[3] Various strategies have been explored to develop hydrogels loaded with antibiotics, growth factors,[4] anti-inflammatory drugs,[5] and antioxidant drugs[6] to combat the problems in chronic wounds. However, hydrogels prepared by conventional chemically cross-linking methods are mechanically weak and fragile,[7] restricting their application in the stress-loading scenarios of diabetic foot ulcer management. The maximum

[a] Zhejiang International Scientific and Technological Cooperative Base of Biomedical Materials and Technology, Zhejiang Engineering Research Center for Biomedical Materials, Cixi Institute of Biomedical Engineering, Ningbo Institute of Materials Technology and Engineering, Chinese Academy of Sciences, Ningbo 315300, China. E-mail: rong.wang@nimte.ac.cn
[b] School of Mechatronics Engineering, Nanchang University, Nanchang 330031, China. E-mail: dlliu@ncu.edu.cn
[c] School of Materials Science and Engineering, Nanjing University of Science and Technology, Nanjing 210094, China
[d] SSI O V Roman Powder Metallurgy Institute, National Academy of Sciences of Belarus, Minsk, 220005, Belarus

† Electronic supplementary information (ESI) available. See DOI: https://doi.org/10.1039/d1tb02413b

‡ These authors made equal contributions to this work.

plantar pressure and shear stress on the foot of an adult can be as high as 200 kPa and 33 kPa, respectively,[8,9] under which condition most conventional hydrogels are likely to be damaged irreversibly. Recently, hydrogel dressings with high mechanical properties have been developed *via* nanosheet-assembly,[10] interpenetrating network,[11,12] hydrogen bonding cross-linking,[13] and micelle-cross-linking.[14] These hydrogel dressings shine a light on management of the hard-to-heal wounds in a stress-loading environment.

Poly(sulfobetaine methacrylate) (polySBMA) has been widely investigated as wound dressings due to its good hydrophilicity (water absorption and retention properties), tissue adhesiveness (preventing bacterial invasion), antifouling property (inhibiting bacterial adhesion) and biocompatibility. However, conventional polySBMA hydrogel is mechanically weak, and the strategy to improve its toughness is complicated and time-consuming.[15] Tannic acid (TA) is a Generally Recognized As Safety (GRAS) compound approved by the US Food and Drug Administration (FDA) and used as antibacterial and antioxidant agent. As a natural polyphenol compound with numerous phenolic hydroxyl groups, TA can act as hydrogen-donor to form hydrogen bonding with other hydrogen-acceptor groups, and electrostatically interact with ionic polymers upon ionization of the phenol groups.[16] In addition, polyphenols are reported to be effective agents for treatment of chronic wounds because of their multifunctionalities including antioxidant activity, upregulation of pro-healing and anti-inflammatory gene pathways, and prevention of bacterial infection.[17] Attributing to the excellent physico-chemical and biological properties of the TA, various TA-doped hydrogels have been developed as tissue adhesives,[18] hemostatic sealants,[19] and wound dressings.[20]

Herein, a tannic acid-reinforced poly(sulfobetaine methacrylate) (TAPS) hydrogel with high toughness and appropriate bioactivities was developed, which aims at addressing the problems in treatment of chronic diabetic wounds. TA molecules served as physical cross-linkers in polySBMA network to improve the mechanical property of the hydrogel, and as an antioxidant and antibacterial agent to confer it with bioactivity. The mechanical property, tissue adhesiveness, pressure-relieving property, antioxidant and antibacterial property, cytotoxicity of the TAPS hydrogel were investigated. *In vivo* wound healing performance of the TAPS hydrogel was evaluated using a diabetic mouse model.

2 Material and methods

2.1 Materials

[2-(Methacryloyloxy)ethyl]dimethyl-(3-sulfopropyl)ammonium hydroxide (sulfobetaine methacrylate, SBMA, 97%), tannic acid, ammonium persulfate (APS, 98%), 2,2-diphenyl-1-picrylhydrazyl (DPPH, 97%), urea, and agar were purchased from Aladdin Chemistry (Shanghai, China). Poly(ethylene glycol) diacrylate (PEGDA, M_n 550 Da) and streptozotocin were purchased from Sigma-Aldrich (Shanghai, China). Artificial sweat (Catalogue No.: CF-001) was obtained from Chuangfeng Technology (Dongguan, China) and used as received. Tryptic soy broth and lysogeny broth were purchased from Baisi Biotechnology (Hangzhou, China). *Staphylococcus aureus* (*S. aureus*) 5622 was a gift from the Affiliated Hospital of School of Medicine of Ningbo University. The strain was isolated from patients with cutaneous wound infections. *Escherichia coli* (*E. coli*) ATCC 25922 was obtained from American Type Culture Collection. NIH/3T3 fibroblast cells (Catalogue No.: SCSP-515) were obtained from National Collection of Authenticated Cell Cultures, Chinese Academy of Sciences.

2.2 Hydrogel preparation

SBMA solution at a concentration of 4 mol L^{-1} was prepared by dissolving 22.3 g of SBMA monomer in 20 mL deionized water. Subsequently, 0.85 g, 1.69 g, 2.53 g, or 3.38 g of TA (2 wt%, 4 wt%, 6 wt% and 8 wt% of the SBMA solution) was dissolved in the solution. Ninety mg of PEGDA and 23 mg of APS were then added to the solution. The precursor solution was degassed with nitrogen bubbling for 30 min, injected into a silicone-sealed glass mold, and incubated at 60 °C overnight to form hydrogel by free radical polymerization. The resultant hydrogel containing 2 wt%, 4 wt%, 6 wt% and 8 wt% of TA was denoted as TAPS2, TAPS4, TAPS6, and TAPS8 hydrogels, respectively. PolySBMA hydrogel was prepared in a similar manner as described above but without the addition of TA. The prepared hydrogel was frozen in liquid nitrogen and freeze-dried. The cross-section of the hydrogel was observed using scanning electron microscope (SEM, regulus 8230, Hitachi, Japan). Fourier transform infrared (FTIR) spectroscopy measurements of the samples were carried out using a Thermo Scientific Nicolet iS50 spectrophotometer.

2.3 Mechanical property and self-healing capability

To investigate the tensile property, hydrogels were cut into strips (40 mm × 10 mm × 1 mm), and tested in a Universal Testing Machine (CMT-1104, SUST, China) at a crosshead speed of 100 mm min^{-1}. For the compression test, hydrogels were cut into a disk shape (diameter of 9 mm, thickness of 2 mm), loaded in the Universal Testing Machine, and compressed at a crosshead speed of 10% strain per minute until 90% strain. The stress–strain curve was recorded. For the cyclic compression test, the hydrogel disk was compressed until 60% strain and then relaxed at a crosshead speed of 10% strain per minute. The maximum compressive stress at each cycle was recorded. To evaluate the self-healing capability, the hydrogel disk was cut into halves and connected along the gap at 37 °C for 2 h. The compressive stress of the hydrogel after the healing process was evaluated as described above. In the scratch recovery test, the surface of a TAPS8 hydrogel was partially cut to obtain a small scratch, and the recovery of the scratch was recorded using a digital microscope.

2.4 Hydrogel swelling capability

Hydrogels were cut into disks (diameter of 9 mm, thickness of 2 mm), incubated in 15 mL of deionized water, urea solution, NaCl solution, or artificial sweat at 37 °C for a determined period of time. Then, excess water on the surface of the swelled hydrogel was removed by filter paper. The hydrogel before and

after swelling was weighted, and the swelling ratio of the hydrogel was calculated using eqn (1):

$$S = \frac{W_1 - W_0}{W_0} \times 100\% \quad (1)$$

where S is the swelling ratio, and W_0 and W_1 are the weight of the hydrogel before and after swelling, respectively.

The swelled hydrogels were freeze-dried, and the morphology of the cross-section was observed using SEM.

2.5 Surface adhesion property

To demonstrate the universal adhesion property, the hydrogel was applied on the surface of various materials including rubber, wood, glass, and plastic. The adhesive strength of the hydrogel to porcine skin (bought from a local supermarket) was evaluated using the lap shear method following the previous work.[14] All porcine skins were cleaned with deionized water to remove any oily dirt prior to the tests. The adhesion strength of hydrogel to skin tissue was calculated by dividing the maximum fracture force by the contact area of the hydrogel-skin assembly (225 mm^2). The stability of the adhesion property was investigated by covering the hydrogel on a breach of a glove (made of nitrile butadiene rubber), which was then filled with water.

2.6 Foot pressure measurement

Hydrogel (2 mm in thickness) was cut into a disk shape with a diameter of 20 mm, and a thin-film pressure sensor (DF9-40, Leanstar Electronic, Suzhou, China) was placed on top of it. An adult ($\sim$65 kg) was standing on the hydrogel-sensor assembly. The pressure on the pelma was recorded and calculated following the manufacturer's instructions. The pressure on the subject's pelma without hydrogel was measured using the same sensor.

2.7 TA release from hydrogel

Hydrogel disks (diameter of 9 mm, thickness of 2 mm) were incubated in 2 mL of phosphate-buffered saline (PBS, 10 mM, pH 7.2 or 5.0) in a 24-well plate. After a determined period, 900 μL of PBS was withdrawn from the well and replaced with the same amount of fresh PBS. The UV absorbance of the collected solution was measured at 280 nm using a UV-Vis spectrometer (TU-1810, Persee, China), and the concentration of TA released to PBS solution was calculated from the standard curve. Cumulative release of TA was obtained by summing up the release amount at every time point.

2.8 Antioxidant capacity

Fifty mg of hydrogel was placed in 3 mL of DPPH solution (0.1 mM in ethanol). The solution containing hydrogel was incubated at room temperature under darkness for a determined period of time, and the absorbance of the DPPH solution at 517 nm was recorded. The radical scavenging rate of the hydrogel was calculated using the eqn (2):

$$R = \frac{A_0 - A_1}{A_0} \times 100\% \quad (2)$$

where R is the free radical scavenging rate, and A_0 and A_1 are the absorbance of the DPPH solution at 517 nm before and after reaction with hydrogel.

2.9 Antibacterial test

Bacteria were cultured in designated culture broth (tryptic soy broth for *S. aureus* and lysogeny broth for *E. coli*) at 37 °C overnight with shaking at 100 rpm. The bacterial culture was diluted using sterilized PBS (10 mM, pH 7.2) by 1000 times. A hydrogel disk (diameter of 9 mm, thickness of 2 mm) was placed in 5 mL of the bacterial suspension, incubated at 37 °C with shaking. Bacterial PBS suspension without hydrogel was set as the control group. After 6 h, viable bacterial cells in the suspension were counted using the spread plate method as described in the previous study.[14]

2.10 Cytotoxicity assay

Cytotoxicity test was conducted according to the standard ISO-10993-5[21] with slight modification using NIH/3T3 fibroblasts. Cells in Dulbecco's modified Eagle's medium (DMEM, Hyclone, supplemented with 10% fetal bovine serum, 1.0×10^5 U L^{-1} penicillin, and 100 mg L^{-1} streptomycin) were seeded in 96-well plate with a density of 10^4 cells per well and cultured in DMEM at 37 °C with 5% CO_2 for 24 h. All hydrogel samples were sterilized under UV light for 30 min, and then 500 mg of the hydrogels were incubated in 8 mL of deionized water at 37 °C for 24 h. The obtained extract solution of the hydrogels was mixed with DMEM at a volume ratio of 1 : 9. Then, culture medium in the cell culture plate was replaced with the mixture of extract solution and DMEM. Solutions of deionized water/DMEM mixture, full fresh medium, medium containing 10 mg mL^{-1} of zinc diethyldithiocarbamate were included as controls. After 24 h, cell counting kit-8 (CCK-8, TransGen Biotech Co., Ltd, China) assay was used to evaluate the cell viability following the manufacturer's protocol. Cell viability was expressed as the percentages of absorbance value of experimental group relative to that of the negative control group (deionized water/DMEM mixture).

2.11 Skin irritation and wound healing evaluation

ICR mice were housed and fed in the Animal Center of Ningbo University according to the protocol approved by the Institutional Animal Ethics Committee of Ningbo University. Animal irritation test of the hydrogels was conducted using ICR male mice (25–30 g) according to the standard ISO 10993-10 as described in the previous study.[14] The skin appearance of the hydrogel application site at 0, 1, 24, 48, and 72 h after the hydrogel removal was recorded. The *in vivo* skin wound healing capability of hydrogel was evaluated using streptozotocin-induced diabetic ICR mice. Briefly, diabetes was induced in ICR mice using streptozotocin following an established protocol.[4] Full-thickness wounded sites of 12 mm diameter were created on the back of the diabetic mouse, followed by covering with polySBMA or TAPS8 hydrogel disk (diameter of 9 mm, thickness of 1 mm). For the control group, the wound site was left without any treatment. A 3M™ Tegaderm™ dressing was then covered on the wound. On days 0, 2, 4, 7, 14, 21, the

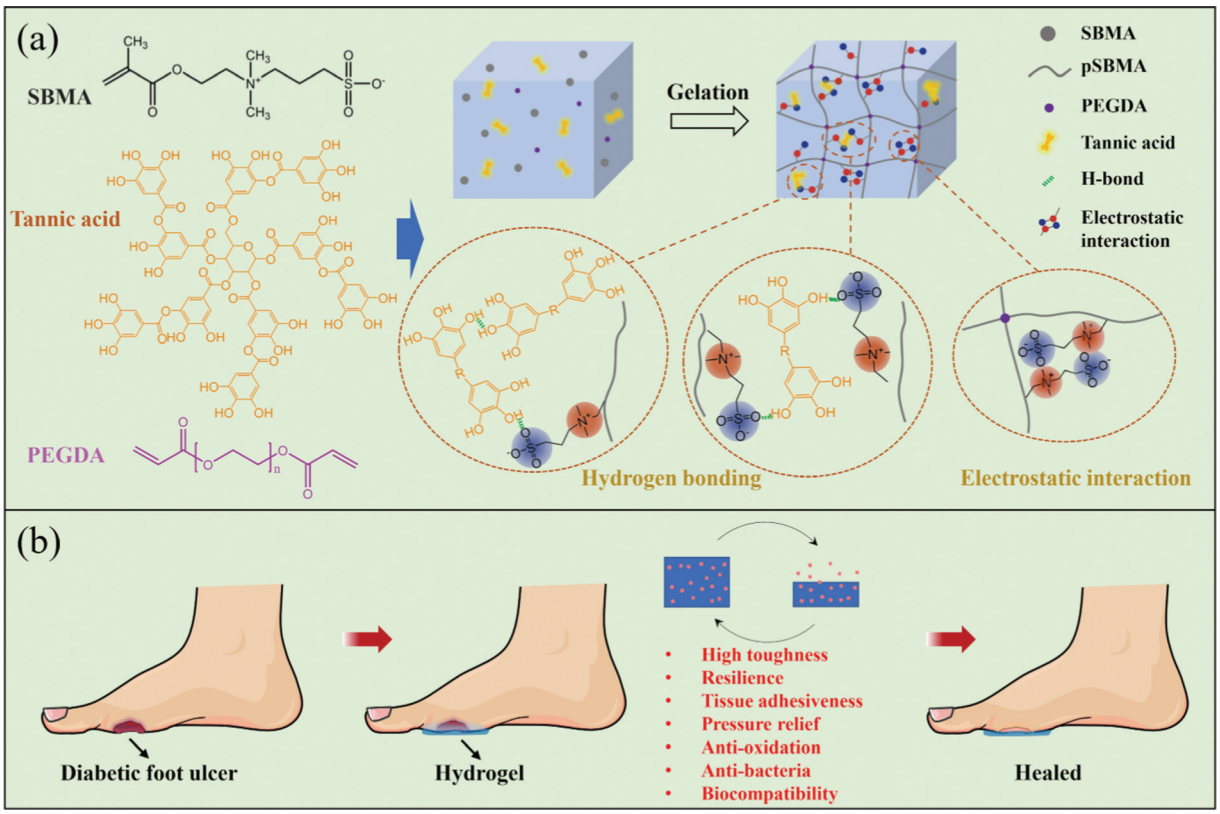

Scheme 1 Schematic illustration of (a) preparation of TA-reinforced polySBMA hydrogels with multiple hydrogen bonding and electrostatic interactions, and (b) proposed applications of TAPS hydrogel for treatment of diabetic foot ulcer.

wound area was observed and measured using ImageJ (version 1.52p). The mice were sacrificed and the tissue at the wound site was stained using hematoxylin and eosin (H&E, Solarbio G1120, China). Histological observation of the stained tissue was carried out using an inverted microscope equipped with a digital camera (DFC450 C, Leica, Germany). Assessment of degree of inflammation of the wound tissues was performed blindly by a pathologist. At least three mice were used for each group.

2.12 Statistical analysis

The results were reported as mean ± standard deviation from at least three samples from each group. Student's *t*-test or one-way analysis of variance (ANOVA) with Tukey test were applied to determine the statistical significance (accepted at $p < 0.05$) between various groups.

3 Results and discussion

3.1 Fabrication of TA-reinforced hydrogel

The TAPS hydrogel was fabricated *via* a facile and straightforward one-step free-radical polymerization of SBMA, with PEGDA as the chemical cross-linker, and TA as the non-covalent cross-linker (Scheme 1). Zwitterionic polySBMA, considering its strong electrostatic! interaction, desirable wound healing capability, and biocompatibility,[14,15] was chosen to form a primary covalent network. As shown in Fig. S1 (ESI†), FTIR spectra of SBMA and TA + SBMA revealed the appearance of peaks at 1635 cm^{-1} and 963 cm^{-1} that are corresponding to the stretching vibration of C═C and C═C–H bonds in SBMA monomer, respectively. The disappearance of these peaks in polySBMA, TA + polySBMA, TAPS8 samples indicated the successful free radical polymerization of SBMA monomer. In the spectrum of TA, the adsorption bands at 1196 cm^{-1}, 1612 cm^{-1}, and 1717 cm^{-1} were caused by stretching vibration of C_{Ar}–O, C–O, and C═O bonds, respectively, and broad adsorption at 3000–3700 cm^{-1} was present due to the large amount of C_{Ar}–OH. The peak shifted to 3445 cm^{-1} in TAPS8, indicating the formation of hydrogen bonding between TA and polySBMA network. The spectrum of TAPS8 showed high similarity to that of the mixture of TA and polySBMA (TA + polySBMA), confirming only physical interaction formed between TA and polySBMA.

A typical single network of polySBMA hydrogel is mechanically weak with tensile fracture stress and ultimate compressive stress of 42.2 kPa and 1.4 MPa, respectively (Fig. 1a and b). TA containing abundant phenolic hydroxyl groups, which could serve as donors in hydrogen bonding formation,[22,23] was introduced into the polySBMA network. The polyphenols interact with polySBMA chains *via* hydrogen bonding and electrostatic interactions, forming multiple physically cross-linked points in the network (Scheme 1). The TA-reinforced zwitterionic hydrogel with an increasing amount of TA showed a dense structure with fewer cracks at the cross-section compared with polySBMA hydrogel (Fig. 1d). The tensile stress of the TAPS hydrogel

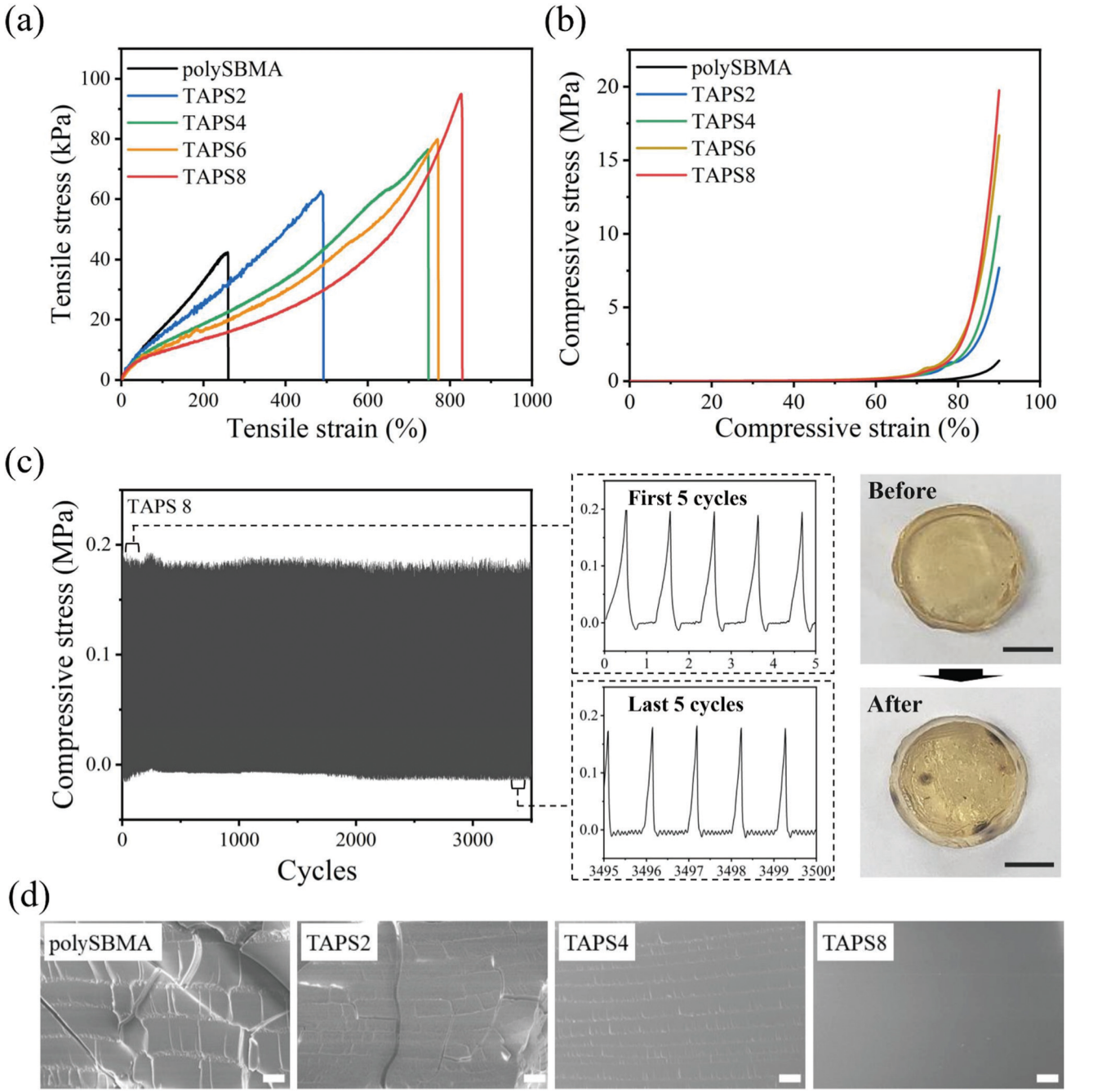

Fig. 1 (a) Representative tensile stress–strain curves and (b) compressive stress–strain curves of polySBMA hydrogel and TAPS hydrogels. (c) Compressive stress of TAPS8 hydrogel over 3500 cycles, and the digital photos of TAPS8 hydrogel before and after the 3500 compression cycles. (d) SEM images of the cross-section of as-prepared polySBMA hydrogel and TAPS hydrogels. Scale bars in (c and d) represent 5 mm and 10 μm, respectively.

increased from 62.6 kPa of TAPS2 hydrogel to 93.7 kPa of TAPS8 hydrogel (Fig. 1a). The maximum plantar shear stress in diabetic patient is reported to be 33 ± 9 kPa.[9] Therefore, it is expected that the TAPS hydrogels could resist the shear stress on foot and maintain its integrity in the application. The compressive stress of the hydrogel was significantly increased with the addition of TA in the network, from 9.8 MPa of TAPS2 to 18.4 MPa of TAPS8 (Fig. 1b). The ultimate compressive stress of TAPS hydrogel, as well as the increased ratio of compressive stress compared with pristine polySBMA hydrogel (up to 13.1-fold), is higher than the value of the previously reported TA-impregnated hydrogels.[24] This is probably due to that the hydrogen bonding between TA and polymer chains is homogeneously distributed in the TAPS hydrogel network, thus providing strong and reversible interaction to dissipate external energy efficiently.[25] In addition, the non-covalent cross-linking structure of hydrogen bonding and electrostatic interactions imparted the TAPS hydrogel with excellent self-healing

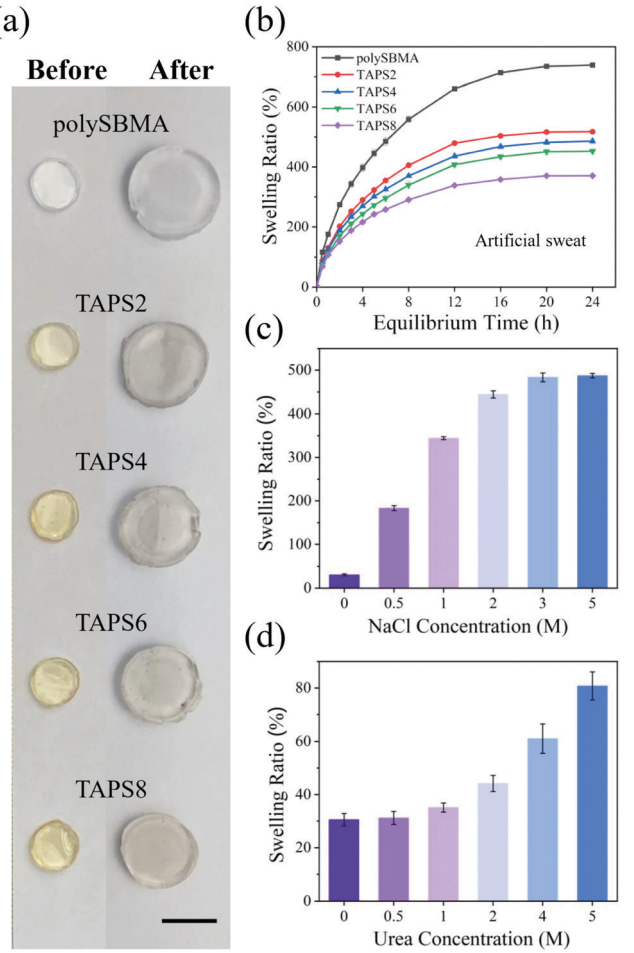

Fig. 2 (a) Digital photos of polySBMA and TAPS hydrogels before and after swelling in artificial sweat for 5 h. Scale bars represent 1 cm. (b) Swelling behavior of polySBMA and TAPS hydrogels in artificial sweat over 24 h. Swelling behavior of TAPS8 hydrogel in (c) NaCl solution and (d) urea solution after 24 h.

capability. Two pieces of TAPS8 hydrogels healed together within 5 min (Fig. S2a, ESI†). When the TAPS8 hydrogel was cut into halves, and then healed at 37 °C for 2 h, its compressive stress recovered to 16.5 MPa (~90% of its original value). Noticeable healing activity of the TAPS8 hydrogel was observed within 9 min in the surface scratch recovery test (Fig. S2b, ESI†). Upon cyclic compressive loading/unloading of TAPS8 hydrogel at 60% strain for up to 3500 cycles, the hydrogel maintained good integrity and showed a stable compressive stress of ~200 kPa over the compression cycles (Fig. 1c). This value is as high as the reported maximum in-shoe plantar pressure of an adult (~200 kPa).[8] The excellent mechanical property, self-healing, and resilience properties of the hydrogel make it a good candidate as wound dressing to withstand the plantar pressure and shear stress in diabetic foot treatment.

3.2 Swelling property

The swelling property of dressings is important in wound management to absorb wound exudate and maintain a moist microenvironment.[26] All the hydrogels prepared in this study swelled after incubating in artificial sweat or deionized water for 5 h (Fig. 2a and Fig. S3a, ESI†). The polySBMA hydrogel showed an excellent swelling property in artificial sweat, with a swelling ratio of 739% after 24 h of incubation (Fig. 2b). Introduction of TA inhibited TAPS hydrogel swelling due to the dense cross-linking structures in the network. The equilibrated swelling ratio of TAPS2 hydrogel in artificial sweat was 518%, and it further reduced to 371% in TAPS8 hydrogel. The cross-section of swelled polySBMA, TAPS2, and TAPS4 hydrogels showed porous structures, and the pore size gradually decreased with increase of the concentration of TA (Fig. S3b, ESI†). TAPS6 and TAPS8 hydrogels showed a compact structure even after swelling, which is probably due to the high degree of physical crosslinking between TA and polySBMA chains. Artificial sweat contains a high amount of NaCl and urea. Therefore, TAPS8 hydrogel was further incubated in NaCl solution and urea solution individually to investigate the effect of ions and urea molecules on hydrogel swelling behavior. As can be seen, with increasing concentrations of NaCl and urea, the hydrogel swelled to a larger extent (up to 487.3% and 80.8%, respectively, Fig. 2c and d). This confirmed the important roles of electrostatic interactions and hydrogen bonding in maintaining the structural integrity of hydrogel. When TAPS8 hydrogel was incubated in NaCl solution, Na^+ and Cl^- ions shielded the zwitterionic groups on the polymer chains, thereby resulting in a reduction of electrostatic interactions. Similarly, urea molecule, as a strong hydrogen bonding-formation agent, would destruct the hydrogen bonding between the polymer chains, and cause a looser polymer network. It could be anticipated that the contribution of electrostatic interactions and hydrogen bonding in the hydrogel network is considerable since the swelling achieved an equilibrium state at a high concentration of NaCl/urea.

3.3 Adhesion property

Hydrogels with reliable and suitable adhesion to tissues offer a favorable property for wound healing application as they could prevent bacterial invasion and maintain a good moisture condition.[27] The TAPS hydrogel exhibited a universal and robust adherent property to various materials including rubber, wood, glass, and plastic (Fig. 3a). The adhesive strength of the hydrogels on porcine skin was evaluated using lap shear test (Fig. 3b). PolySBMA hydrogel adhered to tissue due to the dipole–dipole interactions between the zwitterionic groups and the charged groups on the skin surface.[14] The introduction of TA in polySBMA hydrogels significantly promoted the adhesive strength, which increased from 6.0 kPa of TAPS2 to 20.2 kPa of TPAS8 (Fig. 3c). This value is higher than that reported using fibrin glue (3–10 kPa) which is clinically used in wound closure.[28,29] The good tissue adhesiveness ensures the TAPS hydrogel has good conformal cutaneous deployment and resists the shear stress on foot when it is used in combination with an adhesive film, and it could be easily peeled off without any residues (Fig. 3d). In addition to the interaction between zwitterionic groups and skin, the multiple hydrogen bonding

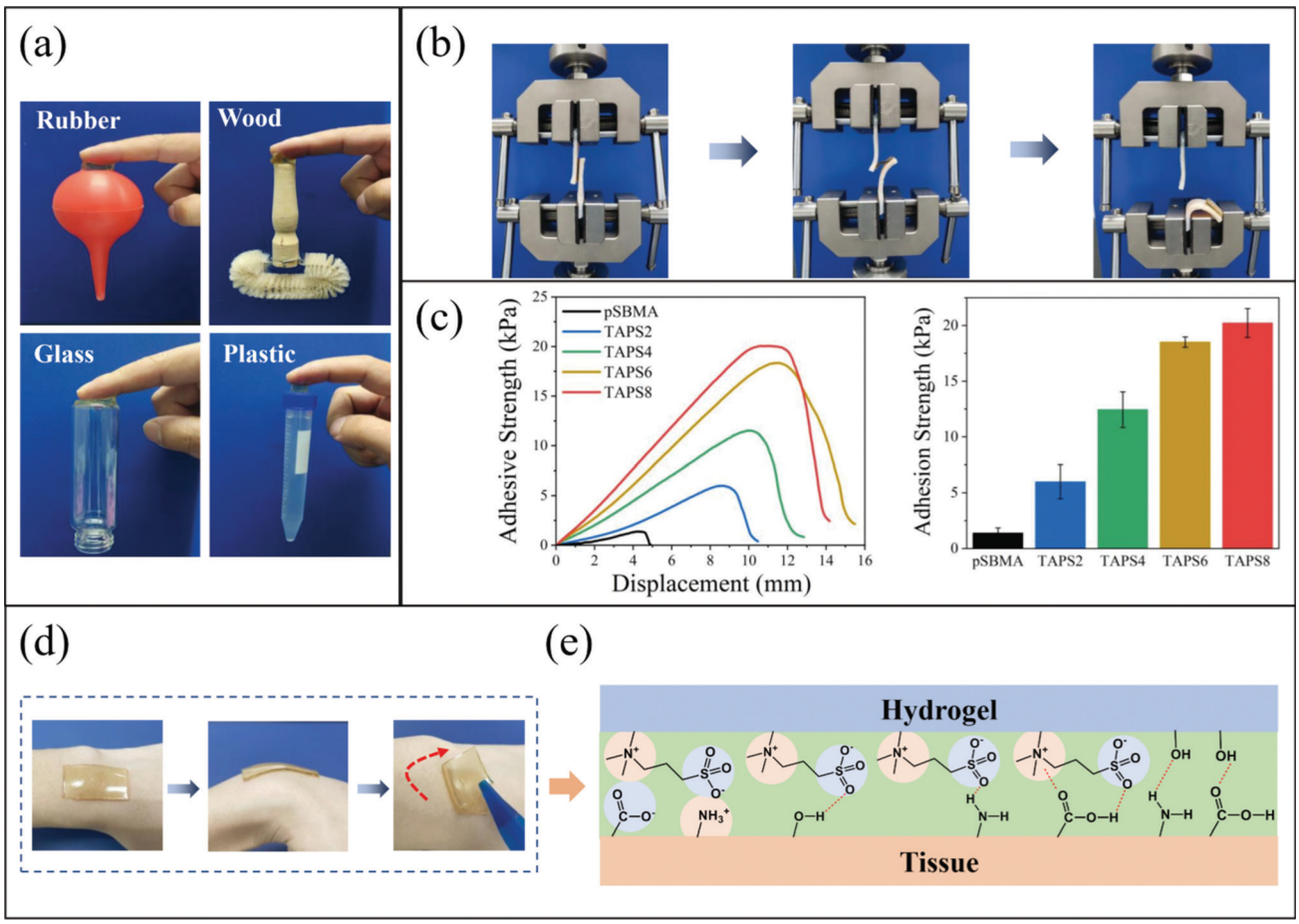

Fig. 3 (a) Digital photos of TAPS8 hydrogel adhered to rubber, wood, glass, and plastic. (b) Digital photos of the lap shear test. (c) Representative adhesive strength–displacement curves, and adhesion strength of the hydrogels to porcine skin. (d) Digital photos of a TAPS8 hydrogel adhering on skin. (e) Possible adhesion mechanisms between the hydrogel and tissue.

between polyphenol groups and the skin could also contribute to the robust adhesion property to the skin (Fig. 3e).[30] Note that after completely swelled, the hydrogel showed limited adhesive property due to hydration of zwitterionic groups and disruption of hydrogen bonding. In the actual scenario for wound treatment, the hydrogel dressing covers the wound bed as well as the surrounding intact skin, and the exudate secreting from the wound bed is continuously absorbed by the hydrogel. To mimic such a condition, a TAPS8 hydrogel was covered on the breach of a glove (made of nitrile butadiene rubber), which was then filled with water (Video S1, ESI†). The hydrogel adhered firmly to the glove and prevented water leakage over 48 h, without showing dehydration (Fig. S4, ESI†). This indicated the hydrogel is applicable as a wound dressing that could adhere to the wounded site and absorb wound exudate.

3.4 Relief of plantar stress

Hydrogels with various forms such as injectable gel,[4] sprayable liquid,[31] and scaffold[32] have been developed and explored their applications in foot ulcer treatment. While most studies focus on the antibacterial and wound healing performance, little effort has been dedicated to investigation of the pressure-relieving property of hydrogel dressings. Excessive plantar stress is one of the major reasons resulting in new and recurrent foot ulcers.[2] Mechanical forces could alter the microenvironment of the wound bed, causing alteration in cellular function, motility and signalling through various mechanotransduction pathways,[33,34] inducing cell apoptosis or necrosis,[35] thereby impeding the healing process. Pressure off-loading has been reported to be an effective treatment for healing the wound and preventing the reoccurrence of diabetic foot ulcers.[36] Elastic materials such as micro-cellular rubber, silicone have been used to construct pressure-relieving insoles.[37,38] Soft hydrogels that were able to distribute stress at the wound site have shown good performance in neovascularization, cell proliferation and polarization of M2/M1 macrophages, and consequently high wound healing efficiency.[39] In this study, the performance of the TAPS hydrogel in relieving plantar pressure was evaluated using a customized pressure-sensing setup (Fig. 4a). As can be seen, the pressure on areas which usually experiences high plantar stress (site a, area below the first metatarsal head, and site b, area below the calcaneus) has been reduced by 12.9% and 27.5%, respectively, after application with a TAPS8 hydrogel (Fig. 4b). The good pressure-relieving property of TAPS hydrogel is in good agreement

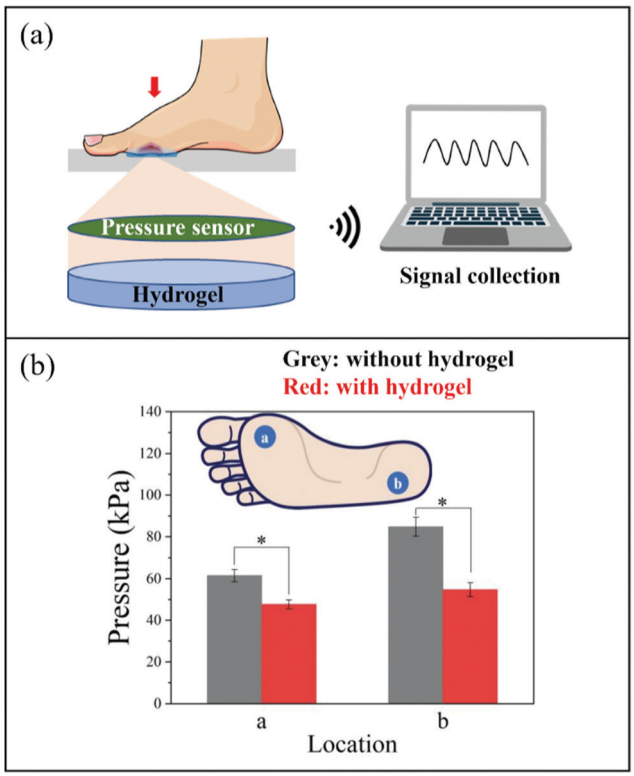

Fig. 4 (a) Schematic illustration of the setup used for plantar pressure measurement. (b) Plantar pressure with and without application of a TAPS8 hydrogel (2 mm in thickness, and diameter in 20 mm). * denotes statistically significant difference with $p < 0.05$ between the two groups.

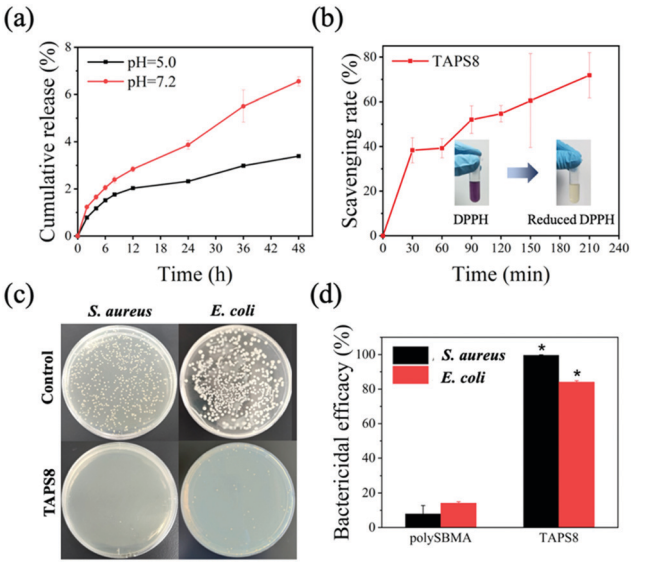

Fig. 5 (a) Cumulative release of TA from TAPS8 hydrogel in PBS with different pH values. (b) The radical scavenging rate of TAPS8 hydrogel in DPPH solution. Inset: DPPH solutions before and after reacting with TAPS8 hydrogel. (c) Digital photos of survival bacteria (*S. aureus* and *E. coli*) clones on culture plates after incubating with TAPS8 hydrogel for 6 h. (d) Bactericidal efficacy of TAPS8 hydrogel against *S. aureus* and *E. coli* after incubation in PBS for 6 h. * denotes statistically significant difference with $p < 0.05$ between the TAPS8 group and polySBMA group.

with the excellent mechanical property and resilience as discussed above, and is likely to be beneficial for healing of diabetic foot ulcers.

3.5 TA release and antioxidant capacity

Chronic wound, such as diabetic foot ulcer is hard to heal due to the elevated level of local oxidative stress. Persistent inflammatory response at the wound leads to accumulation of reactive oxygen species (ROS), which hinders the transition of inflammation phase to proliferation phase, and delays or even prevents the healing process.[40] TA is a well-known natural antioxidant with good biocompatibility.[41] It is expected that the non-covalent bonded TA molecules could release from the hydrogel and act as a radical scavenger to promote the healing process. TA can be oxidized into quinones under alkaline conditions while maintain its protonated/deprotonated forms under mild acidic to neutral conditions.[22,42] It was found that at pH of 5.0 and 7.2, the release rate of TA was stable and sustainable (Fig. 5a), and ~3.4% and ~6.6% of TA in the TAPS8 hydrogel released over 48 h, respectively. A higher release rate of TA at pH 7.2 compared to that at pH 5.0 was observed. This is probably because, at pH 7.2, there is a relatively larger proportion of deprotonated TA molecules that are dissociated due to disruption of the hydrogen bonding, release from the hydrogel network. The radical scavenging capability of TA-releasing hydrogel was evaluated using DPPH method. As can be seen, the scavenging rate was 38.3% at 30 min, and increased to 71.8% at 210 min (Fig. 5b), indicating the rapid and strong radical scavenging ability of the TAPS hydrogel. The TA-releasing hydrogel with good radical scavenging capability is promising for chronic wound treatment.

3.6 Antibacterial property

Bacterial infection is a major hindrance to the wound healing process. The hydrogels were incubated with wound-relevant bacteria to evaluate their antibacterial efficacy. The polySBMA hydrogel exhibited limited bactericidal activity,[43] while the TAPS8 hydrogel exhibited high bactericidal properties with the killing efficacy of 99.6% and 84.0% against *S. aureus* and *E. coli*, respectively (Fig. 5c and d). The result demonstrated that TA played a primary role in killing bacterial cells. The antibacterial efficacy of TA against *S. aureus* (Gram-positive) was higher than that of *E. coli* (Gram-negative), which was consistent with the previous report.[44] This is probably because TA molecule targets the peptidoglycan in the cell wall to destroy the bacterial integrity,[45] and in Gram-negative bacteria, the TA-peptidoglycan interaction is inhibited by the outer lipid membrane on the cell wall.

3.7 Cytotoxicity and skin compatibility

The cytotoxicity test has been conducted according to the standard ISO-10993-5 with slight modification. As shown in Fig. S5 (ESI†), polySBMA hydrogel showed good cytocompatibility with cell viability of 106%. TAPS2 hydrogel also exhibited high cell viability of about 90%. Increasing the TA content in

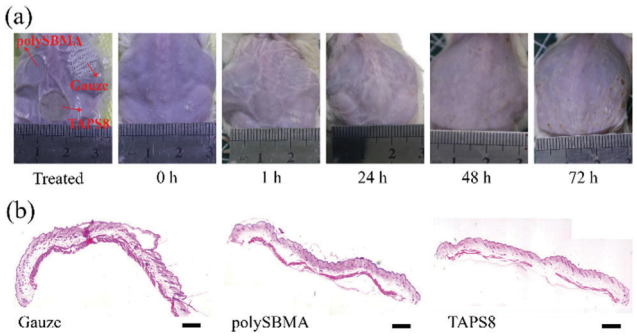

Fig. 6 (a) Representative photos of the appearance of mouse skin that was challenged by gauze (with PBS), polySBMA hydrogel, and TAPS8 hydrogel. Time represents the period after the gauze/hydrogel was removed. (b) H&E staining images of the treated skin areas. Scale bars represent 100 μm.

the hydrogels yielded a small decrease of cell viability from 90% for TAPS2 to 75% for TAPS8 hydrogel, probably due to the dose-dependent inhibition of TA on fibroblast proliferation.[46]

Skin compatibility of the polySBMA and TAPS8 hydrogels was evaluated using the irritation test according to the standard protocol. No reaction signs of erythema or edema were observed on the animal skin after treatment (Fig. 6a). The histological evaluation shows the challenged skin tissue in all groups was intact without any inflammation (Fig. 6b), indicating the hydrogel has good compatibility to skin tissue. According to the irritation score, the hydrogel samples showed negligible irritation on mice skin (Table S1, ESI†). The low cytotoxic effect and the minimal skin irritation showed the hydrogels are biocompatible to be used as wound dressings.

3.8 Wound healing property

To evaluate the wound healing capacity, TAPS8 hydrogel was applied to full-thickness skin defects of diabetic ICR mice for up to 21 days. The wound appearance was recorded and shown in Fig. 7a. From day 2 on, a decrease of wound area showed up in the TAPS8 group, and on day 7, wound area of the TAPS8 group was reduced to 45.1%, compared to that of 79.1% in the control group and 49.3% in the polySBMA group (Fig. 7b). On day 14, the wound area of the TAPS8 group was further reduced to 11.0%. On day 21, almost a full coverage of newborn hair was observed in the TAPS8 hydrogel group. Histological observation of the wounded tissue on days 4, 7, 10 and 21 was recorded (Fig. 7c), and the degree of inflammation on the wound beds was analysed following the method reported in a recent study (Fig. S6, ESI†).[47] On day 4, wound beds in all groups remained open, and mild to severe degree of inflammatory response was present. On day 7, granulation tissue was formed in all groups. A larger gap in the wound area was observed in the control

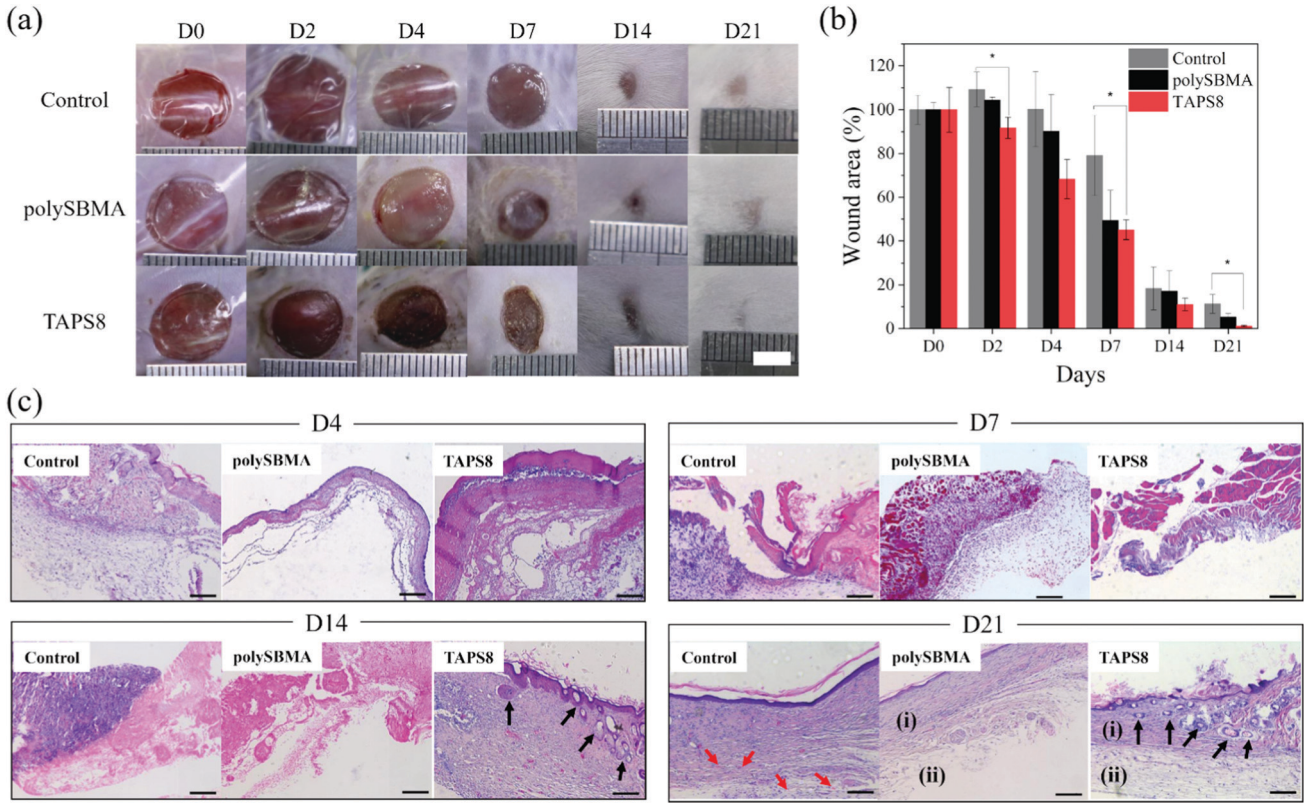

Fig. 7 (a) Representative photos of skin wounds, (b) quantification of the wound area, and (c) H&E staining images of wound beds of the polySBMA hydrogel treated group, TAPS8 hydrogel treated group, and control group. * denotes statistically significant difference with $p < 0.05$ between the two groups. Scale bars in (c) represent 50 μm. Areas of (i) and (ii) in (c) indicate the newly formed dermis and subcutaneous tissues, respectively. Red arrows indicate the inflammatory cells, and black arrows indicate the newly formed hair follicles in the wound area.

group compared to the TAPS8 hydrogel group, indicating the wound was far from closure. On day 14, mitigation of tissue inflammation was observed on the wound treated with TAPS8 hydrogel (Fig. S6, ESI†). Skin structure was forming, the wound bed was closing, and initial re-epithelization and neovascularization were observed (Fig. 7c). However, the wound remained unclosed in the control and polySBMA groups. On day 21, the inflammation degree of the wound was significantly lower in the polySBMA group and TAPS8 group compared to the control (Fig. S6, ESI†). Re-epithelization has been completed at the wound site in the hydrogel groups and the control group. But only in the TAPS8 hydrogel group, clear structures of dermis and subcutaneous tissues and new hair follicles were present, while a large infiltration of inflammatory cells was seen in the dermis in the control group on day 21 (Fig. 7c). In summary, the prepared TAPS8 hydrogel showed a good healing capability for diabetic wounds. It should be noted that no mechanical stimulation was applied on the wound that usually occurred in diabetic foot ulcers, due to the limitation of the animal wound model. Since the hydrogels showed good pressure-relieving capability, it is reasonable to expect that the hydrogel is promising for treatment of wounds such as diabetic foot ulcers exposing to a stress-loading environment.

4 Conclusions

In this study, a mechanically reinforced hydrogel with multiple biofunctionalities was developed *via* a straightforward fabrication strategy of incorporating TA in zwitterionic polySBMA hydrogel. The TAPS hydrogel exhibited excellent mechanical property and tissue adhesiveness, attributed to the formation of multiple non-covalent interactions between TA and zwitterionic polymer chains. Due to the good mechanical properties and adhesiveness, the hydrogel reduced the plantar stress on foot. In addition, the hydrogel sustainably releases TA, and subsequently eliminated endogenous ROS and killed both Gram-positive and Gram-negative bacteria efficiently. *In vivo* and *in vivo* studies confirmed that the hydrogel had low cytotoxicity and a minimal irritant effect on mouse skin, and effectively promoted wound healing in a diabetic mouse model. In summary, this work developed a mechanically tough hydrogel with desirable bioactivities for effectively addressing the problems in stress-relevant chronic wounds, thus providing a promising solution for the treatment of difficult-to-heal diabetic wounds.

Author contributions

K. Fang and Q. Gu developed the basic concept, conducted the experiments of hydrogel preparation and characterization, analyzed the data and wrote the manuscript. M. Zeng and Z. Huang performed the hydrogel characterization and analysis of experiment. M. Zeng, H. Qiu, J. Miao and Y. Fang conducted the animal experiment and analyzed the data. Y. Zhao, Y. Xiao, and T. Xu assisted in conducting the experiments and analysis of data. R. P. Golodok, V. V. Savich, A. P. Ilyushchenko and F. Ai contributed to review and editing the manuscript. D. Liu contributed to supervision, review and editing the manuscript. R. Wang contributed to development of the basic concept, supervision, review and editing the manuscript.

Conflicts of interest

There are no conflicts of interest to declare.

Acknowledgements

This work was funded by the National Key Research and Development Program of China (2018YFE0119400), National Natural Science Foundation of China (51803229, 52011530019), Youth Innovation Promotion Association CAS (2021296), S&T Innovation 2025 Major Special Program of Ningbo (2018B10040), Natural Science Foundation of Zhejiang Province (LQ21E030006), Ningbo Public Welfare Science & Technology Major Project (2021S106), and Ningbo Clinical Medicine Research Center Project (2019A21003). The authors thank Professor Chunnian Wang from Ningbo Clinical Pathology Diagnosis Center for the histological assessment.

References

1 NCD Risk Factor Collaboration, *The Lancet*, 2016, **387**, 1513–1530.
2 D. G. Armstrong, A. J. M. Boulton and S. A. Bus, *N. Engl. J. Med.*, 2017, **376**, 2367–2375.
3 H. Wang, Z. Xu, M. Zhao, G. Liu and J. Wu, *Biomater. Sci.*, 2021, **9**, 1530–1546.
4 H. Zhao, J. Huang, Y. Li, X. Lv, H. Zhou, H. Wang, Y. Xu, C. Wang, J. Wang and Z. Liu, *Biomaterials*, 2020, **258**, 120286.
5 E. Mauri, A. Rossetti, P. Mozetic, C. Schiavon, A. Sacchetti, A. Rainer and F. Rossi, *Eur. J. Pharm. Biopharm.*, 2020, **146**, 143–149.
6 G. Cirillo, M. Curcio, U. G. Spizzirri, O. Vittorio, P. Tucci, N. Picci, F. Iemma, S. Hampel and F. P. Nicoletta, *Eur. Polym. J.*, 2017, **90**, 1–12.
7 S. Fuchs, K. Shariati and M. Ma, *Adv. Healthcare Mater.*, 2020, **9**, e1901396.
8 J. Park, M. Kim, I. Hong, T. Kim, E. Lee, E. A. Kim, J. K. Ryu, Y. Jo, J. Koo, S. Han, J. S. Koh and D. Kang, *Sensors*, 2019, **19**, 5504.
9 J. E. Perry, J. O. Hall and B. L. Davis, *Gait Posture*, 2002, **15**, 101–107.
10 L. Yan, T. Zhou, L. Han, M. Zhu, Z. Cheng, D. Li, F. Ren, K. Wang and X. Lu, *Adv. Funct. Mater.*, 2021, **31**, 2010465.
11 J. Li, A. D. Celiz, J. Yang, Q. Yang, I. Wamala, W. Whyte, B. R. Seo, N. V. Vasilyev, J. J. Vlassak, Z. Suo and D. J. Mooney, *Science*, 2017, **357**, 378–381.
12 X. Chen, H. Yuk, J. Wu, C. S. Nabzdyk and X. Zhao, *Proc. Natl. Acad. Sci. U. S. A.*, 2020, **117**, 15497–15503.

13 C. Fan, B. Liu, Z. Xu, C. Cui, T. Wu, Y. Yang, D. Zhang, M. Xiao, Z. Zhang and W. Liu, *Mater. Horiz.*, 2020, **7**, 1160–1170.
14 K. Fang, R. Wang, H. Zhang, L. Zhou, T. Xu, Y. Xiao, Y. Zhou, G. Gao, J. Chen, D. Liu, F. Ai and J. Fu, *ACS Appl. Mater. Interfaces*, 2020, **12**, 52307–52318.
15 X. Li, C. Tang, D. Liu, Z. Yuan, H. C. Hung, S. Luozhong, W. Gu, K. Wu and S. Jiang, *Adv. Mater.*, 2021, **33**, e2102479.
16 H. Liang, B. Zhou, D. Wu, J. Li and B. Li, *Adv. Colloid Interface Sci.*, 2019, **272**, 102019.
17 J. B. Johnson, D. A. Broszczak, J. S. Mani, J. Anesi and M. Naiker, *J. Pharm. Pharmacol.*, 2022, **74**, 485–502.
18 Y. Yang, X. Zhao, J. Yu, X. Chen, R. Wang, M. Zhang, Q. Zhang, Y. Zhang, S. Wang and Y. Cheng, *Bioact. Mater.*, 2021, **6**, 3962–3975.
19 Z. Qiao, X. Lv, S. He, S. Bai, X. Liu, L. Hou, J. He, D. Tong, R. Ruan, J. Zhang, J. Ding and H. Yang, *Bioact. Mater.*, 2021, **6**, 2829–2840.
20 Z. Ahmadian, A. Correia, M. Hasany, P. Figueiredo, F. Dobakhti, M. R. Eskandari, S. H. Hosseini, R. Abiri, S. Khorshid, J. Hirvonen, H. A. Santos and M. A. Shahbazi, *Adv. Healthcare Mater.*, 2021, **10**, e2001122.
21 ISO 10993-5: 2009. Biological Evaluation of Medical Devices—Part 5: Tests for *in vitro* cytotoxicity, 2009.
22 L. Q. Xu, K.-G. Neoh and E.-T. Kang, *Prog. Polym. Sci.*, 2018, **87**, 165–196.
23 Z. Guo, W. Xie, J. Lu, X. Guo, J. Xu, W. Xu, Y. Chi, N. Takuya, H. Wu and L. Zhao, *J. Mater. Chem. B*, 2021, **9**, 4098–4110.
24 B. Liu, Y. Wang, Y. Miao, X. Zhang, Z. Fan, G. Singh, X. Zhang, K. Xu, B. Li, Z. Hu and M. Xing, *Biomaterials*, 2018, **171**, 83–96.
25 P. Lin, S. Ma, X. Wang and F. Zhou, *Adv. Mater.*, 2015, **27**, 2054–2059.
26 N. R. Barros, S. Ahadian, P. Tebon, M. V. C. Rudge, A. M. P. Barbosa and R. D. Herculano, *Mater. Sci. Eng., C*, 2021, **119**, 111589.
27 Y. Yi, C. Xie, J. Liu, Y. Zheng, J. Wang and X. Lu, *J. Mater. Chem. B*, 2021, **9**, 8739–8767.
28 J. Chen, J. Yang, L. Wang, X. Zhang, B. C. Heng, D.-A. Wang and Z. Ge, *Bioact. Mater.*, 2021, **6**, 1689–1698.
29 L. Wang, X. Zhang, K. Yang, Y. V. Fu, T. Xu, S. Li, D. Zhang, L. N. Wang and C. S. Lee, *Adv. Funct. Mater.*, 2019, **30**, 1904156.
30 C. Cui, C. Shao, L. Meng and J. Yang, *ACS Appl. Mater. Interfaces*, 2019, **11**, 39228–39237.
31 J. Ouyang, X. Ji, X. Zhang, C. Feng, Z. Tang, N. Kong, A. Xie, J. Wang, X. Sui, L. Deng, Y. Liu, J. S. Kim, Y. Cao and W. Tao, *Proc. Natl. Acad. Sci. U. S. A.*, 2020, **117**, 28667–28677.
32 Y. Li, T. Xu, Z. Tu, W. Dai, Y. Xue, C. Tang, W. Gao, C. Mao, B. Lei and C. Lin, *Theranostics*, 2020, **10**, 4929–4943.
33 B. Kuehlmann, C. A. Bonham, I. Zucal, L. Prantl and G. C. Gurtner, *J. Clin. Med.*, 2020, **9**, 1423.
34 L. A. Barnes, C. D. Marshall, T. Leavitt, M. S. Hu, A. L. Moore, J. G. Gonzalez, M. T. Longaker and G. C. Gurtner, *Adv. Wound Care*, 2018, **7**, 47–56.
35 L. Wang, J. Pan, T. Wang, M. Song and W. Chen, *PLoS One*, 2013, **8**, e75973.
36 S. A. Bus, *Plast. Reconstr. Surg.*, 2016, **138**, 179S–187S.
37 A. K. Mishra, R. Kumar, C. Kataria, S. Goel, A. Verma and A. K. Sinha, *J. Clin. Med. Res.*, 2020, **2**, 1–17.
38 H. Jiang, M. Ochoa, V. Jain and B. Ziaie, *MRS Commun.*, 2018, **8**, 1184–1190.
39 H. He, Z. Xiao, Y. Zhou, A. Chen, X. Xuan, Y. Li, X. Guo, J. Zheng, J. Xiao and J. Wu, *J. Mater. Chem. B*, 2019, **7**, 1697–1707.
40 Z. Xu, S. Han, Z. Gu and J. Wu, *Adv. Healthcare Mater.*, 2020, **9**, e1901502.
41 J. Yeo, J. Lee, S. Yoon and W. J. Kim, *Biomater. Sci.*, 2020, **8**, 1148–1159.
42 G. Ghigo, S. Berto, M. Minella, D. Vione, E. Alladio, V. M. Nurchi, J. Lachowicz and P. G. Daniele, *New J. Chem.*, 2018, **42**, 7703–7712.
43 R. Wang, K. G. Neoh and E. T. Kang, *J. Colloid Interface Sci.*, 2015, **438**, 138–148.
44 B. Kaczmarek, *Materials*, 2020, **13**, 3224.
45 G. Dong, H. Liu, X. Yu, X. Zhang, H. Lu, T. Zhou and J. Cao, *Nat. Prod. Res.*, 2018, **32**, 2225–2228.
46 D. Pattarayan, A. Sivanantham, R. Bethunaickan, R. Palanichamy and S. Rajasekaran, *J. Cell. Biochem.*, 2018, **119**, 6732–6742.
47 H. Yuk, J. Wu, T. L. Sarrafian, X. Miao, C. E. Varela, E. T. Roche, L. G. Griffiths, C. S. Nabzdyk and X. Zhao, *Nat. Biomed. Eng.*, 2021, **5**, 1131–1142.

